Applied Catalysis B: Environmental 121–122 (2012) 214–222

Contents lists available at SciVerse ScienceDirect

Applied Catalysis B: Environmental

journal homepage: www.elsevier.com/locate/apcatb

Effect of Fe–olivine on the tar content during biomass gasification in a dual fluidized bed

M. Virginie[a], J. Adánez[b], C. Courson[a,*], L.F. de Diego[b], F. García-Labiano[b], D. Niznansky[c], A. Kiennemann[a], P. Gayán[b], A. Abad[b]

[a] Laboratoire Matériaux, Surfaces et Procédés pour la Catalyse UMR 7515, 25, rue Becquerel, 67087 Strasbourg, France
[b] Instituto de Carboquímica (ICB-CSIC), Department of Energy and Environment, Miguel Luesma Castán, 4, 50018 Zaragoza, Spain
[c] Department of Inorganic Chemistry, Faculty of Natural Sciences of Charles University, Albertov 6, 128 43 Prague 2, Czech Republic

ARTICLE INFO

Article history:
Received 2 February 2012
Received in revised form 3 April 2012
Accepted 4 April 2012
Available online 11 April 2012

Keywords:
Fe/olivine catalyst
Biomass gasification
Tar removal
Dual fluidized bed

ABSTRACT

The Fe/olivine catalyst effectiveness regarding tar primary reduction during biomass gasification in dual fluidized beds has been investigated. The use of Fe/olivine instead olivine leads to an important decrease in the amount of produced tar, which was reduced by up to 65% at 850 °C, naphthalene being the most stable molecule. It has been found that Fe/olivine materials have a double effect on tar destruction. On the one hand, they act as a catalyst for tar and hydrocarbon reforming. On the other hand, they can act as an oxygen carrier that transfers oxygen from the combustor to the gasifier, and part of the oxygen is used to burn volatile compounds. The catalyst was fairly stable because the result was confirmed during 48 h of continuous operation. The Fe/olivine material characterization (X-ray diffraction, Mössbauer spectroscopy, temperature programmed reduction and oxidation, etc.) revealed that the catalyst structure was maintained despite the large number of oxidizing–reducing cycles. The carbon that formed on the catalyst surface was low and easily oxidized in the combustion zone. Therefore, the inexpensive and non-toxic Fe/olivine catalyst is a material suitable for use as primary catalyst in a fluidized bed gasification of biomass.

© 2012 Elsevier B.V. All rights reserved.

1. Introduction

Biomass gasification is an interesting technology in future development of a worldwide sustainable energy system, which can help to decrease our current dependence on fossil fuels. Biomass gasification is a thermal process where solid fuel is converted into a useful gas using several gasifying agents such as air, and steam. The producer gas has a great number of applications. The most important being combustion for power and heat generation as well as raw gas for production of fuels or chemicals [1].

There are several designs of small and large scale gasifiers available for the use of biomass. Among them, those based on fluidized bed technology offer several advantages including the possibility of being scaled up to both medium and large scale, and temperature limitation to avoid bed agglomeration [2]. Moreover, the use of some specific designs can present additional advantages. For example, the use of a dual fluidized bed gasification system can be used to generate a high quality producer gas. The steam blown dual fluidized bed reactor located at Güssing is a well-known example of the successful industrial application of this technology [3]. The basic idea behind this gasification system is to physically separate the gasification and the combustion reactions, in order to obtain a largely nitrogen-free producer gas. Both reactors are thermally connected due to a circulating bed material. The gasification of biomass takes place in a steam fluidized bed. Together with the circulating bed material, ungasified char is transported to the combustion reactor and burned with air. Heat is delivered back to the gasifier by the bed material to satisfy the endothermic gasification reactions.

However, gasification produces not only useful fuel gases but also some unwanted byproducts. Among them, tar is recognized as one of the most problematic parameters in any gasification system [4,5]. Most of the tar removal technologies are based on low temperature gas cleaning processes located downstream to the gasifier [6]. Among hot gas conditioning systems, catalytic cracking and steam reforming of high molecular weight hydrocarbons offer several advantages, such as thermal integration and high tar conversion. A large number of investigations deal with biomass gasification in fluidized bed reactors utilizing nickel based catalysts, dolomite or olivine. Supported nickel-based catalysts with various supports and promoters have been the most widely studied class of materials. The high activity and selectivity of those reforming catalysts is well known [7,8] but they are susceptible to deactivation from contaminants. Olivine shows a slightly lower

* Corresponding author. Tel.: +33 368852770; fax: +33 368852768.
E-mail address: claire.courson@unistra.fr (C. Courson).

0926-3373/$ – see front matter © 2012 Elsevier B.V. All rights reserved.
http://dx.doi.org/10.1016/j.apcatb.2012.04.005

Table 1
Proximate and ultimate analysis of pine wood.

Property	Parameter value (wt%)
Total moisture	6.30
Ash	1.10
Volatiles content	77.30
Fixed carbon	15.40
C	46.60
H	6.00
N	0.20
S	0.004
Cl	0.002
High heating value (kJ/kg)	18,235

activity in biomass gasification and tar reforming, but higher attrition resistance than dolomite [9]. The addition of some metals to olivine can help to increase its tar reforming activity. In this sense, the tar abatement activity of a Ni/olivine catalyst was successfully demonstrated in the 100 kWth FICFB (dual fluidized bed steam blown biomass gasifier) pilot plant located in Vienna, with an order of magnitude reduction in the tar content of the product fuel gas [10,11]. The main drawback attributed to the use of Ni is the cost and the environmental and safety measures derived from its toxicity.

In addition, Rauch et al. [12] demonstrated that olivine activity, or more specifically olivine activation, depends on its iron oxide content. In fact, depending on olivine temperature treatment, iron can be present in the olivine phase, or as iron oxides. Thus, iron impregnation of natural olivine appears to be very interesting way to produce in-bed primary catalysts, for both economic and environmental reasons. Iron does not affect the catalyst cost due to its low price in comparison to noble metals and nickel thus markedly reducing catalyst pollution problems.

A global objective of this work was: (a) to develop a new material, the Fe/olivine prepared by impregnation; (b) to test its capacity for a primary in-bed reduction of heavy hydrocarbons (tar) in a dual fluidized bed gasification system; and (c) to characterize the material after the tests to determine its behavior during long term operation.

Point (a) has been studied and detailed in a previous paper [13], where the Fe/olivine catalyst preparation, characterization before testing and preliminary reaction of toluene steam reforming have been largely discussed. The aim of the present paper is focused on both points (b) the Fe/olivine efficiency in tar removal in a dual fluidized bed and (c) after testing characterizations.

2. Experimental

2.1. Biomass

The biomass feedstock consisted of crushed and sieved pine wood with average particle size of 0.5–2.0 mm. Proximate and ultimate analysis of the biomass is given in Table 1. The applied feedstock is characterized by low ash, nitrogen, sulfur and chlorine contents. Thus, possible undesirable effects on the in situ catalysts (deactivation caused by sulfur) might be avoided.

2.2. Preparation of Fe/olivine catalysts

The olivine used in this study came from Austria (Magnolithe GmbH) and its mechanical resistance has been improved by calcination at 1600 °C for 4 h. Olivine is a silicate mineral in which magnesium and some iron cations were embedded in the silicate tetrahedral. The elemental analysis performed by ICP-MS on this mineral allows the determination of its composition: 30.5 wt% Mg–19.6 wt% Si–7.1 wt% Fe. Mössbauer spectroscopy, associated to X-ray diffraction, revealed that half of the 7.1 wt% Fe is present as Fe(III) oxides (α-Fe_2O_3, $MgFe_2O_4$) and the other part is present as Fe(II) inside the olivine structure. The Fe(III)/Fe(II) ratio depends on the calcination conditions [13,14].

The Fe/olivine catalyst has been synthesized using an optimized method of impregnation. Iron nitrate ($Fe(NO_3)_3{\cdot}9H_2O$), in an appropriate quantity to assure an additional iron content of about 10 wt%, was dissolved in an optimized amount of water by heating. About 25 kg of olivine (100–250 μm) was added to the iron aqueous solution and the water excess was evaporated under vacuum by heating at 90 °C. The sample was dried inside the tank, then overnight under an extractor hood, before being calcined at 1000 °C over 4 h (temperature heating rate of 3 °C min^{-1}). ICP-MS measurements performed after catalyst synthesis indicate a total iron weight percentage of 16 wt% corresponding to the iron initially present in olivine and the added iron.

2.3. Catalysts characterization

X-ray diffraction (XRD) patterns were acquired with a Bruker AXS-D8 advance using Cu Kα radiation, the diffraction spectra have been indexed in comparison to the JCPDS files (Joint Committee on Powder Diffraction Standards).

The Mössbauer spectra measurements were carried out in transmission mode with ^{57}Co diffused into an Rh matrix as a source moving with constant acceleration. The spectrometer (Wissel) was calibrated by means of a α-Fe foil standard, and the isomer shift was expressed with respect to this standard at 293 K. The fitting of the spectra was performed with the help of the NORMOS program.

Temperature programmed reduction (TPR) allows the evaluation of catalyst reducibility by a flow of 3.85% of hydrogen in argon (total flow of 52 mL min^{-1}) on a 50 mg sample. The temperature was increased at a rate of 15 °C min^{-1} from room temperature to 900 °C. A thermal conductivity detector was used to analyze the effluent gas for a quantitative determination of hydrogen consumption.

The amount of carbon deposited on catalyst after the reactivity tests can be determined by the quantification of the oxidation products (CO_2) observed during temperature programmed oxidation (TPO) by a mass spectrometer (Quadrupole Pfeifer Omnistar). This analysis was performed on a 50 mg sample. After desorption with helium at up to 900 °C with a slope of 15 °C min^{-1} then cooled, an oxidizing gas mixture of 10% oxygen in helium (total flow of 50 mL min^{-1}) passed through the catalyst heated up to 1000 °C with a slope of 15 °C min^{-1}. This technique allows to determine the carbon deposition stability depending on the carbon oxidation temperature.

2.4. Description of the bench scale unit

Continuous catalytic steam gasification of biomass has been performed using a bench scale unit based on the dual fluidized bed (DFB) reactor system (Fig. 1) in a temperature range between 750 °C and 850 °C. This process consists of two bubbling interconnected fluidized beds: the gasifier (0.05 m inner diameter and 0.2 m height) and the combustor reactor (0.08 m inner diameter and 0.1 m height). The gasifier and the combustor were externally heated by furnaces for the start-up of the plant, so as to avoid excessive heat loss and to control the temperature in the reactors more efficiently.

Interconnection of the reactors was made by two loop seals and solid materials circulating between the two reactors. Two different fluidized bed materials (olivine and Fe/olivine) with particle size in the range of 0.1–0.25 mm were used. A test with silica sand was

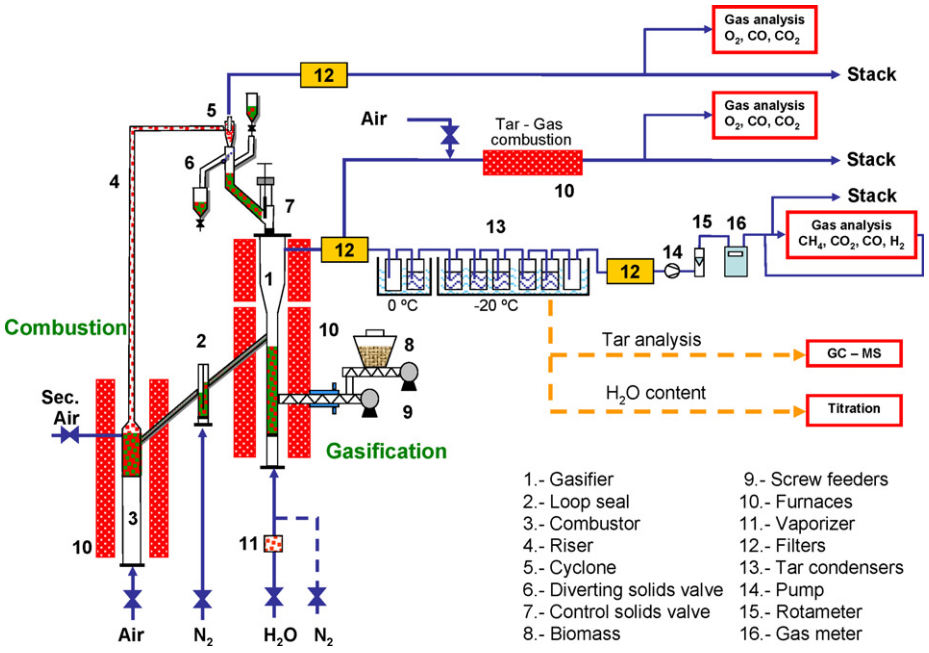

Fig. 1. Scheme of the bench scale gasification unit.

also carried out to compare the effectiveness on the tar reduction of the other bed materials.

The biomass was fed at a rate of 250 g h^{-1} by means of two screw feeders. The first controlled the biomass feeding and the second introduced the biomass as quickly as possible into the gasifier to avoid the pyrolysis in the pipe. The steam/fuel ratio was varied between 0.5 and 0.9.

The solids circulated from the gasifier to the combustor through a fluidized bed loop seal to avoid gas mixing between reactors. In the combustor, the residual char was burned with the combustion air injected at two levels (primary and secondary air). The warm solids were carried through the riser, recovered in a cyclone and returned to the gasifier. A fixed bed acted as the upper loop seal to avoid gas mixing between reactors. It is also possible for the plant to control and measure the solid circulation rate by means of a solids valve.

The flue gas streams from the gasifier and combustor were connected to on-line gas analyzers. Gases such as CO, CO_2 and CH_4 were determined in non-dispersive infrared (NDIR) analyzers, the O_2 in a paramagnetic analyzer, and the H_2 by a thermal conductivity detector. Off-line gas analysis was also carried out in a gas chromatograph fitted with a Porapack N column to analyze the presence of C1–C3 hydrocarbons in the gas outlet stream of the gasifier.

The gas outlet stream from the gasifier had a double way. During non-steady state conditions, the whole stream was burned in a reactor at 900 °C. Only when steady-state conditions were reached, a part of the stream was sent for tar and gas analysis.

The general information concerning the operation and geometry data of the pilot rig are given in Table 2.

2.5. Characterization and quantitative analysis of tars

An off-line method for the sampling and analysis of tars based on the European Tar Protocol [15] was used. Fig. 1 shows a scheme of the tar sampling system. The collection of moisture and tar was performed in a series of 8 impinger bottles by absorption in isopropanol, located in two different cooling baths: the first two impingers at 0 °C and the others six impingers at −18 °C. A cotton filter to further capture the tars escaping from the series of impingers was placed after the last condenser. A flow-meter regulated the gas sampling velocity given by the pump, and the total gas volume was measured in a gas-meter before sending the gas to the analyzers. In all the tests, ≈1 nl min^{-1} of dry gas was drawn through the tar sampling system to reach 60 L of total gas volume.

After the experiment all the samples were mixed thoroughly to insure homogeneity. About 0.7 L of isopropanol containing water and tars was obtained. The water content of the samples was determined using the Karl–Fischer titration method (CRISON Titromatic KF1S). The quantitative determination of the concentrations of the different tar compounds in the samples has been determined by a gas chromatograph (Agilent 7890A) fitted with a capillary column (HP-5) and a flame ionization detector. Furthermore, the GC was coupled with a mass spectrometer (Agilent 5975C). Naphthalene and phenanthrene were selected for the external calibration procedure. The quantitative values were obtained assuming a similar response factor to naphthalene for tar compounds of 1–2 rings and similar to phenanthrene for 3-rings compounds.

Table 2
General operation and geometry data.

Parameter	Unit	
Fuel power	kW	1.5
Feedstock particle size	mm	Up to 2
Bed material particle size range	μm	100–250
Gas residence time in gasifier	s	1.5–2
Solid residence time in gasifier	min	4–6

Parameter	Unit	Gasifier	Combustor
Operable temperature range	°C	750–850	750–900
Fluidization agent		Steam	Air
Volume flow	Nm^3/h	0.10–0.15	1.2–1.5
Fluidization regime		Bubbling fluidized	Bubbling fluidized
Steam/fuel ratio		0.5–0.9	–
Bed height	m	0.2	0.1
Reactor inner diameter	mm	50	80

Table 3
Dry gas composition, tar and water content of biomass gasification performed at different temperatures, in the presence of silica sand, olivine or Fe/olivine.

Test	1	2	3	4	5	6	7	8	9
Bed material	Silica sand	Olivine	Olivine	Olivine	Fe/olivine	Fe/olivine	Fe/olivine	Fe/olivine	Fe/olivine
Gasifier temperature [°C]	800	750	800	850	750	800	800	800	850
Combustor temperature [°C]	900	900	900	900	900	900	900	900	900
Biomass [g h^{-1}]	250	250	250	250	250	250	250	250	250
Steam/biomass ratio[g/g_{db}]	0.60	0.65	0.65	0.62	0.60	0.50	0.60	0.90	0.57
Gasifier									
Gas composition [$vol.\%_{db}$]									
H_2	22.8	26.9	29.2	28.5	29.0	28.4	29.6	31.6	26.7
CO_2	13.2	24.5	27.9	24.8	34.6	22.7	29.6	37.8	41.8
CO	43.3	31.4	27.4	31.8	22.3	39.4	26.2	20.3	18.7
CH_4	14.4	12.0	10.8	10.3	9.9	9.5	10.2	9.2	8.8
C_2H_4	5.2	4.4	3.9	3.9	3.6	–	3.7	1.1	3.2
C_2H_6	0.6	0.5	0.5	0.4	0.4	–	0.4	0.1	0.4
C_3H_8	0.4	0.3	0.3	0.3	0.3	–	0.3	0.1	0.3
Water content [$vol.\%_{db}$]	43.9	47.3	39.6	38.4	45.7	42.9	32.8	47.2	41.4
Tar content [g/Nm^3_{db}]	16.8	8.3	5.5	5.1	5.5	3.9	3.7	4.2	2.6
H_2/CO	0.53	0.86	1.06	0.90	1.30	0.72	1.12	1.56	1.42
Combustor									
Gas composition [$vol.\%_{db}$]									
O_2	18.1	17.2	17.5	17.6	15.7	15.6	16.1	16.4	15.4
CO_2	2.6	2.7	2.4	2.2	3.2	2.7	2.4	2.0	1.8
CO	0.0	0.0	0.0	0.0	0.0	0.0	0.0	0.0	0.0
C_{burned} (%)[a]	21.0	18.5	16.1	13.7	21.9	17.9	17.3	14.7	12.6

[a] Carbon burnt in the combustor with respect to the total carbon fed into the gasifier.

3. Results and discussion

3.1. Biomass gasification tests results

Several gasification tests have been carried out in the gasification plant to analyze the effect of the main operating variables such as the gasification temperature (750–850 °C) and the steam to fuel ratio (0.5–0.9) for different bed materials. The Fe/olivine has been used as bed material in the gasification plant and its activity compared to that of olivine material. A reference test with silica sand was also carried out for comparison reasons. Table 3 shows a summary of the main operating conditions and the results obtained.

The gasification plant was operated during 48 h in different operation conditions. Solid samples were taken from the gasifier and the combustor at different operation times to evaluate the properties of the catalysts along the continuous operation. These samples were characterized by the techniques mentioned above.

Temperature is an important variable regarding gasification. In this study, several experiments were carried at different temperatures ranging from 750 °C to 850 °C using olivine and Fe/olivine as bed materials (Table 3). In all cases, the freeboard temperature was fixed at 800 °C.

The bed material affects both the gas composition and tar yield. Olivine (test 3) and Fe/olivine (test 7) increase H_2 production and decrease CO and CH_4 contents with respect to the use of silica sand (test 1). That implies that H_2/CO ratio increases from 0.53 for silica sand to 1.06 and 1.12 for olivine and Fe/olivine, respectively. However, the most important effect of the bed material is related to the tar content. For a given bed material, higher gasification temperatures produce a decrease in the tar content. It is observed that the use of olivine produces a significant decrease in the amount of tar produced when compared with silica sand (test 1), as a consequence of the catalytic activity of the olivine (test 3). This result is in agreement with data published by other authors [14,16–19].

However, tar reduction was most significant in the presence of Fe/olivine bed material compared with tests carried out in the presence of olivine (5.1 g/Nm^3 and 2.6 g/Nm^3 of tar content for olivine (test 4) and Fe/olivine (test 9) at 850 °C, respectively). These results are in concordance with the biomass gasification tests conducted at the University of Teramo with the same Fe/olivine bed material [20] in a dense fluidized bed reactor (tar content of 3.7 g/Nm^3 and 1.7 g/Nm^3 for olivine and Fe/olivine, respectively, in a test at a temperature of 800 °C).

In addition, the increase in gasification temperature from 750 °C to 850 °C contributes to the enhancement of the tars removal using Fe/olivine (from 5.5 g/Nm^3 (test 5) to 2.6 g/Nm^3 (test 9)).

Fig. 2 shows a comparison of the main (poly) aromatic tar component levels at the reactor outlet during gasification at 750 °C and 850 °C versus the catalytic material. At all temperatures, the most important aromatic compounds detected were indene and naphthalene. The latter was the most widely produced and also highly stable. Consequently, it was the most difficult to remove. Benzene concentration, important at 750 °C for Fe/olivine, largely decreased at 850 °C. Oxygenate aromatics have never been observed.

An additional operating variable was the steam to biomass (dry basis) ratio. Table 3 (tests 6, 7 and 8) shows the results obtained at 800 °C for three different ratios (0.5, 0.6, and 0.9) in presence of the Fe/olivine bed material. The H_2O/biomass ratio should act primarily on the gas composition leading to an increase in the calorific value of the gas produced. An increase in the water feed produced a decrease in the CO volume percentage, while those of H_2 and CO_2 increased. This change in composition is probably due to the increase in the water gas shift reaction [21–23] (Eq. (1)) with that of the H_2O/biomass ratio. In fact, the H_2/CO ratio increases from 0.72 to 1.56 with an increase in water/biomass ratio from 0.5 to 0.9.

$$CO + H_2O \leftrightarrow H_2 + CO_2 \quad (1)$$

A decrease in the CH_4 and C2–C3 compounds amount, indicating their steam reforming, is observed with the increase in H_2O/biomass ratio from 0.6 to 0.9 (Table 3). However, increasing the water content has a slight effect on the tar reduction (3.7 g/Nm^3 to 4.2 g/Nm^3 for steam/biomass ratio from 0.5 to 0.9), as mentioned in several studies [24–26]. The tar compounds repartition and concentration are similar at each experienced steam/biomass ratio (Fig. 3).

It is known that iron present in olivine and Fe/olivine materials has catalytic activity for tar and hydrocarbon reforming. However, it was interesting to know if other effects were also responsible for

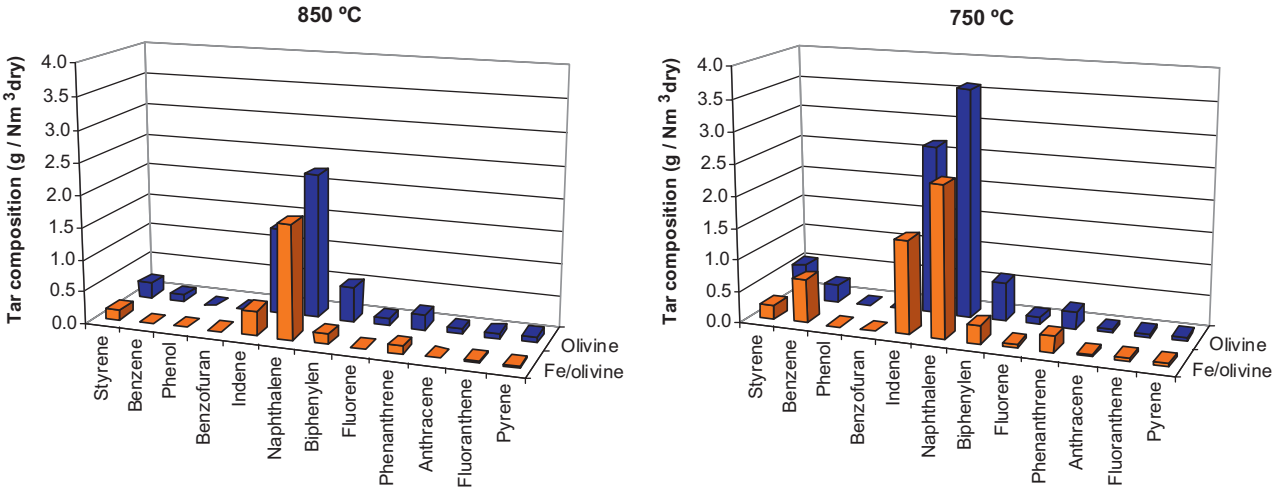

Fig. 2. Effect of solid material on tar composition at T_{gasif} = 750 °C and 850 °C.

the important tar reduction observed in the experimental tests with the Fe/olivine material. For that, mass balances to the system were carried out to determine the oxygen transport process which took place from the combustor to the gasifier at the different operating conditions. The capacity of olivine as the oxygen carrier has been previously shown by Koppatz et al. [27] in a gasifier of similar design used in this work. In addition, iron compounds are usually used as oxygen carriers in chemical-looping processes due to their capacity to be reduced and oxidized in different conditions [28].

The oxygen transport in every test was calculated as the difference between the oxygen fed to the combustor and the oxygen present at the outlet stream as O_2, CO, and CO_2 (see Table 3). The dilution of the stream with the N_2 proceeding from the loop-seal and the solid circulation rate have also been considered for the mass balance. Fig. 4 shows the oxygen transport as a function of the temperature for the different bed materials.

It is observed that the silica sand has not any transport capacity. The olivine presented some capacity for oxygen transport, as reported in previous works [27,28]. The most interesting is the result obtained with the Fe/olivine material where an important effect regarding oxygen transport was detected.

To conclude, it can be said that olivine and Fe/olivine materials have a double effect on tar destruction. On the one hand, they act as a catalyst for tar and hydrocarbon reforming. On the other hand, they can act as an oxygen carrier that transfers oxygen from the combustor to the gasifier and part of the oxygen is used to burn volatile compounds.

3.2. Catalysts characterization

The Fe/olivine catalyst has been characterized before testing and the full characterizations are published elsewhere [13,29]. The XRD indicated that the olivine structure was not modified after 10 wt% iron oxide impregnation and calcination at 1000 °C. The XRD and Mössbauer spectra indicated that the main iron phases present were hematite (α-Fe_2O_3) and spinel ($MgFe_2O_4$). The TPR result demonstrated that a high iron oxide percentage (65%) was reduced [30].

After the experiments, samples from the gasification and combustor reactors have been recovered at different times and characterized to observe the physico-chemical evolution of the iron bulk catalyst during operation in the continuous gasification plant.

The diffractogram of the catalysts coming from the gasification zone at 800 °C (test 7) does not indicate diffraction rays of iron oxide α-Fe_2O_3 (Fig. 5b), as well as no metallic iron diffraction rays. Although, intense diffraction rays of spinel phase ($MgFe_2O_4$, Fe_3O_4) at 2θ = 30.19°, 35.59° and 43.22° are present meaning that in the gasification zone, the iron present is partially reduced. Moreover,

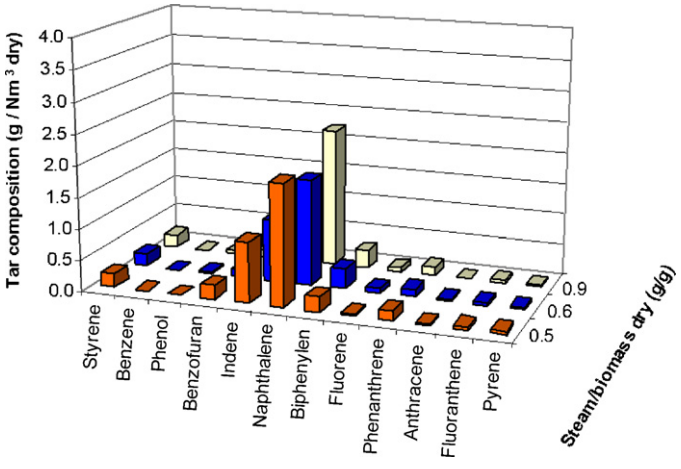

Fig. 3. Effect of H_2O/biomass ratio on tar composition at 800 °C in the presence of Fe/olivine catalyst.

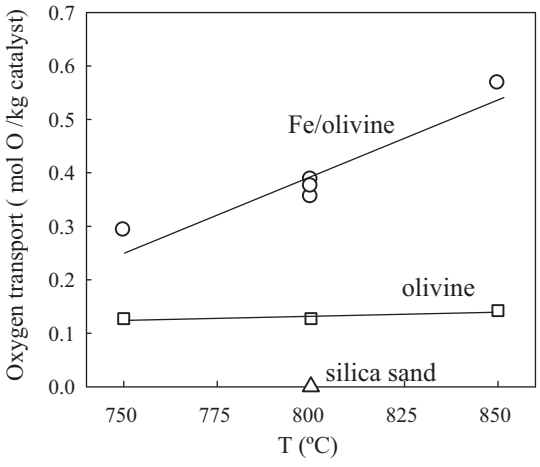

Fig. 4. Oxygen transport process for different bed materials.

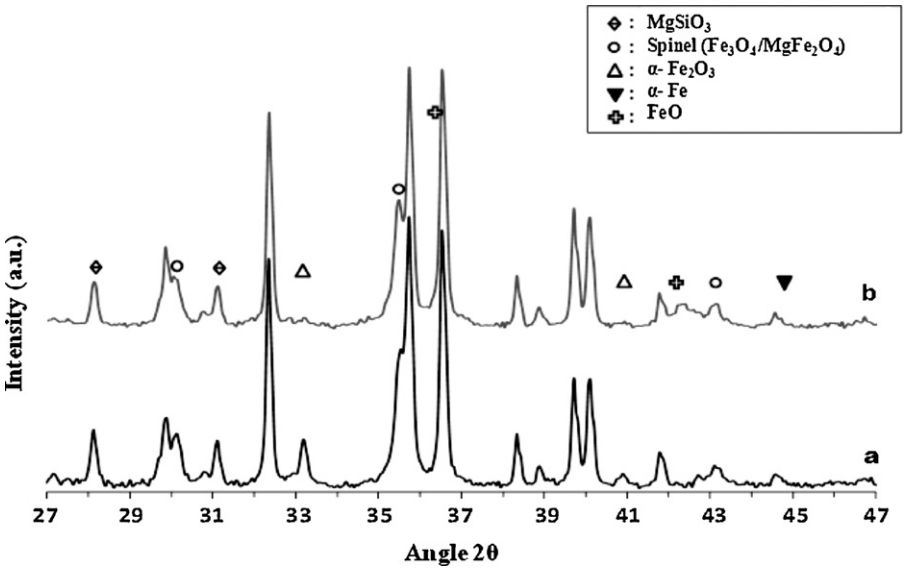

Fig. 5. XRD diffractograms of the Fe/olivine catalyst coming (a) from the combustion zone at 900 °C and (b) from the gasifier at 800 °C, after 16 h of biomass gasification.

after reactivity at 800 °C, small diffraction rays of wustite FeO at $2\theta = 36.32°$ (shoulder) and 42.19° are visible.

The sample coming from the combustion zone (Fig. 5a) has a similar structure than that of the Fe/olivine catalyst before testing. Diffraction rays of iron oxide α-Fe_2O_3 at $2\theta = 33.11°$ and 40.82° and those of spinel phase ($MgFe_2O_4$, Fe_3O_4) are observed. The spinel phase is expected to be $MgFe_2O_4$ due to its presence in the fresh Fe/olivine catalyst calcined under air. This fact demonstrates that Fe/olivine material is fully oxidized in the combustor during every cycle.

The diffractogram (not shown) of the catalyst coming from the gasification zone after the test at 750 °C (test 5) indicates neither diffraction rays of iron oxide α-Fe_2O_3 nor diffraction rays of metallic iron. Intense diffraction rays of spinel phase ($MgFe_2O_4$, Fe_3O_4) have also been observed but no diffraction ray of wustite FeO can be detected. In fact, the gas composition of this test (test 5) contains more CO_2 and H_2O and less CO and CH_4 than during the test at 800 °C (test 7); the atmosphere is then slightly more oxidizing than during the test at 800 °C.

The sample coming from the combustion zone has a similar structure than that of the Fe/olivine catalyst before testing and that of the Fe/olivine catalyst coming from the combustion zone after the gasification test at 800 °C.

From these characterizations, the presence of metallic iron was expected because it is presumed to be active in C—C and/or C—H break bonds [31,32]. However, iron reductions $Fe^{3+} \rightarrow Fe^{2+/3+}$ (Fe_3O_4) and $Fe^{3+} \rightarrow Fe^{2+}$ (FeO) were observed at 750 °C and 800 °C, respectively. It could be supposed that the conditions at the end of the biomass gasification test lead to a partial oxidation of the catalyst, or else the residence time in the gasifier or thermodynamic restrictions does not allow a higher iron reduction in the catalyst bulk [33,34].

The iron distribution is known by the Mössbauer spectroscopy study. After 16 h of gasification testing at 750 °C and 12 h of gasification at 800 °C, the Fe/olivine catalyst was analyzed and the Mössbauer spectra and sub-spectra, resulting from the deconvolution, are shown in Fig. 6. The fitting of the Mössbauer spectrum revealed the presence of two doublets and three sextets.

The doublet D1 with an isomer shift δ equal to 1.14 mm s^{-1} and a quadrupole splitting Δ equal to 2.98 mm s^{-1} is due to Fe^{2+} ions in the olivine structure [35,36]. The doublet D2 with an isomer shift δ equal to 1.05 mm s^{-1} and a quadrupole splitting Δ equal to 0.92 mm s^{-1} is due to Fe^{2+} of wustite FeO [37].

The isomer shift, quadrupole splitting and hyperfine field of the sextet S1 ($\delta = 0.36$ mm s^{-1}, $\Delta = -0.20$ mm s^{-1} and $H_{eff} = 517$ kG) correspond to the Fe^{3+} ions present in α-Fe_2O_3 oxide (hematite) [37,38]. The Mössbauer parameters of the sextets S2 ($\delta = 0.30$ mm s^{-1}; $\Delta = 0$ mm s^{-1} and $H_{eff} = 489$ kG) and S3 ($\delta = 0.36$ mm s^{-1}, $\Delta = -0.20$ mm s^{-1} and $H_{eff} = 517$ kG) are attributed to the presence of Fe^{3+} and Fe^{2+} in tetrahedral sites and octahedral sites of the spinel Fe_3O_4 [37,39,40], respectively.

After the integration of the different subspectra (doublets and sextets), the relative distribution of iron in different phases has been determined and is reported in Table 4.

An important amount of iron (18–21%) returns inside the olivine structure as iron(II) after the gasification tests. This iron reintegration is due to the olivine thermodynamic equilibrium [13,14,41,42]. This material tries to reach an equilibrium structure, with iron content, in function of the temperature and the reductive conditions. Wustite phase, FeO, hardly visible by XRD, is detected and

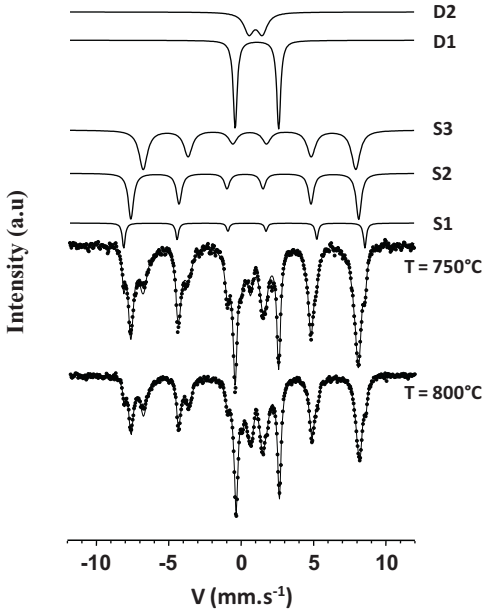

Fig. 6. ^{57}Fe Mössbauer spectra of the Fe/olivine catalyst after gasification tests at 750 °C and 800 °C; subspectra (D: doublet; S: sextet) are indicated at the top.

Table 4
Relative distribution of different phases of iron after the integration of different sub-spectra.

	Fe^{2+} (olivine)	Fe^{2+} (FeO)	$Fe^{2+/3+}$ (Fe_3O_4)	Fe^{3+} (α-Fe_2O_3)	Fe^{3+} ($MgFe_2O_4$)
Before test[a]	8	0	0	33	59
After gasification test at 750 °C	18	11	64	7	0
After gasification test at 800 °C	21	21	52	6	0

[a] Results of the Fe/olivine catalyst prepared in laboratory scale.

quantified after tests at 750 °C and 800 °C. Mössbauer spectroscopy confirms the X-ray diffraction observations indicating the presence of significant Fe_3O_4 spinel phase. Approximately 6–7% of total iron is not reduced in the gasification reactor and remains as α-Fe_2O_3 oxide. As in XRD, the presence of metallic iron Fe^0 or iron carbide (Fe—C) is not revealed by Mössbauer spectroscopy in the catalyst bulk.

During biomass gasification, the catalyst has to circulate from the gasification zone (where iron is partially reduced) to the combustion zone (the iron is oxidized by air). The produced gas composition in the gasifier (Table 3) is not reductive enough to allow iron reduction until the metallic oxidation state. At 800 °C, the gas mixture composition is richer in H_2, CO and CH_4 than at 750 °C. This induces a slight increase in reduced iron (up to 21% FeO) associated with a lower tar concentration.

The iron distribution in the samples after gasification shows a balance between the phases FeO and Fe_3O_4, which provide for tar reforming. Those iron species take place in the redox equations of the water gas shift reaction (Eqs. (2) and (3)):

$$Fe_3O_4 + CO \leftrightarrow CO_2 + 3FeO \quad (2)$$

$$3FeO + H_2O \leftrightarrow H_2 + Fe_3O_4 \quad (3)$$

In the previously stated conditions, the couple $Fe^{2+/3+}/Fe^{2+}$ is sufficiently efficient in tar reforming, without the presence of Fe^0. Several researches based on tars cracking from pyrolysis, from biomass gasification [22,24] or based on tar models molecules steam reforming [33,43,44], in the presence of iron catalysts, have different views on the most active iron oxidation state: Fe^0, Fe^{2+} or $Fe^{2+/3+}$.

Di Felice et al. [33,43] have observed a toluene conversion range of 50–60% at 850 °C with the use of a 5%Fe/(CaMg)O, 5%Fe/CaO or 5%Fe/MgO catalyst. They concluded that the iron couple Fe^{2+}/Fe^{3+}, in cooperation with CaO and MgO and even in the form of FeO–MgO solid solution, is active in the toluene steam reforming reaction.

Polychronopoulou et al. [44] have obtained 63.3% of phenol conversion with 5%Fe/(50% MgO–50%CeO_2) catalyst and 61% of conversion with 5%Fe/(40%CeO_2–60%Al_2O_3) catalyst. They concluded that iron(II) specie is stable in the phenol steam reforming reaction.

Matsuoka et al. [22] and Uddin et al. [24] have considered tars cracking in the presence of water with Fe/Al_2O_3 iron oxide catalysts. They concluded that in the presence of Fe_3O_4 spinel oxide, tars can be reformed.

Fukase and Suzuka [45] have observed a deactivation of iron oxide catalysts in oxidation–reduction cycles of residual oils cracking in the presence of water. They correlated this deactivation to an accumulation of the FeO species, leading to an agglomeration particle. They concluded that a balance between FeO and Fe_3O_4 is essential to prevent catalyst deactivation.

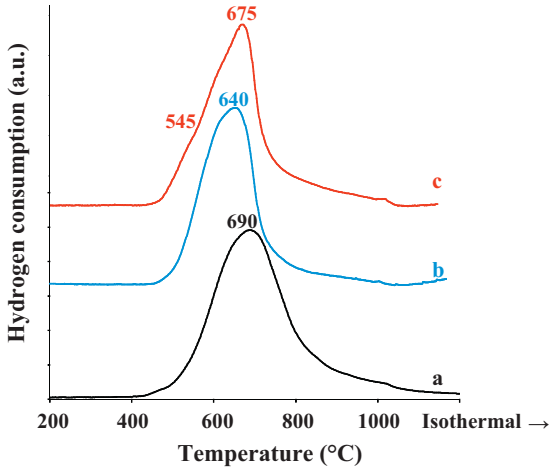

Fig. 7. TPR profiles of the Fe/olivine catalyst (a) before and after (b) 12 h, (c) 48 h of biomass gasification.

However, the research carried out by Nordgreen et al. [34,46], based on different iron oxides activities in tars cracking in the presence of water, have shown up to 20% of additional tars reduction with metallic iron rather than with FeO–Fe_3O_4 species.

On the basis of the literature and of our results, we propose that tar reduction can occur without Fe^0 specie but with the latter, the reaction is improved. The gas composition in the gasifier has an important influence on the oxidation state of iron present on the catalyst.

In order to evaluate the catalyst state after several circulations between the gasifier and the combustor, iron elemental analyses were also performed on the samples coming from the combustion zone (oxidation at 900 °C), tested during 12 and 48 h in biomass gasification (Table 5). An iron loss of 32% has been observed after 12 h of gasification, then, between 12 and 48 h, 17% of iron is lost. This indicates that in dual fluidized bed gasification reactor, the Fe/olivine catalyst has loss a part of its iron content due essentially to attrition phenomena. It can be noticed that the decrease is more important during the first 12 h of biomass gasification than during the following 36 h.

The amount of reducible iron is calculated by temperature programmed reduction (TPR) and permits the evaluation of reducible iron present in the sample after 12 or 48 h of biomass gasification. The TPR curve of the fresh catalyst (Fig. 7a) shows a high peak of hydrogen consumption between 500 °C and 850 °C. This zone is attributed to the reduction of iron oxide present inside the olivine grain, in interaction with the olivine grain. Hydrogen diffusion through olivine grain occurs at high temperature; subsequently these iron oxides are reducible at high temperature [13,30]. The curves of the spent Fe/olivine catalysts (Fig. 7b and c) indicate

Table 5
Total iron weight percentage, hydrogen molar consumption (mmol/g_{cat}) and estimation of the reducible iron percentage.

	Fresh catalyst (a)	After 12 h of biomass gasification (b)	After 48 h of biomass gasification (c)
Fe (wt%)	16.0	10.9 (−32%)	9.0 (−17%)
H_2 molar consumption (mmol/g_{cat})	2.77	1.83	1.33
Fe total reducible (%)	65	43 (−34%)	31 (−28%)

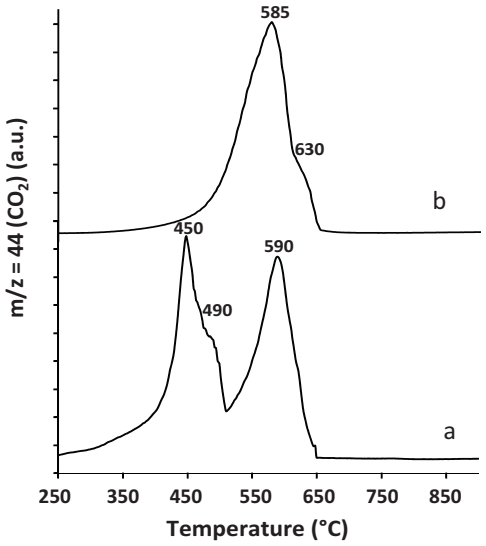

Fig. 8. TPO of the Fe/olivine catalyst after gasification test (a) at 750 °C during 16 h and (b) at 800 °C during 12 h.

a weak shift of hydrogen consumption toward low temperature (between 480 °C and 800 °C). At 545 °C, a shoulder on the curve of the catalyst tested during 48 h (Fig. 7c) is clearly noticeable. This shift may correspond to the migration of a weak part of iron toward the grain surface, reducible at a lower temperature. The decrease in the total iron oxide percentage in the olivine grain could explain the thinner shape of the reduction peak.

After the curves integration, the hydrogen molar consumption has been estimated and the results led to an estimation of the iron reducible percentage after 12 and 48 h of the catalysts reactivity in biomass gasification (Table 5). Compared to the fresh iron catalyst, a decrease in reducibility (the percentage of reduced iron versus total iron) has been observed: 43% and 31% after 12 and 48 h of gasification, respectively.

Between 12 and 48 h of gasification, the loss of iron reducibility (28%) is higher than the loss of iron weight percentage (17%) in the samples which indicates that the narrowing of the reduction peak is not only due to the decrease in the total iron oxide percentage. This difference may be due to the iron reintegration in the olivine structure as Fe(II) which is hardly reducible.

However, the Fe/olivine catalyst remains active in tar reforming (more favorably than olivine) and still participates in the increase in water gas shift reaction.

Knowing that carbon deposit can lead to catalyst deactivation, the amount of carbon deposition has been quantified by temperature programmed oxidation (TPO) performed on the Fe/olivine catalysts coming from the gasification zone after biomass gasification at 750 °C and 800 °C. It is observed that the higher the gasifier temperature, the lower the formation of carbon (given in mole of carbon per gram of the catalyst and per hour for each test in biomass gasification): 1.73×10^{-5} $mol_C/g_{cat}/h$ and 1.60×10^{-3} $mol_C/g_{cat}/h$ of carbon formation at 800 °C and 750 °C, respectively. In both cases the carbon deposition is weak. Nevertheless, it is one hundred times less at 800 °C than at 750 °C.

Different carbon species have been detected (Fig. 8) on these samples according to the position of the carbon oxidation peaks.

The catalyst from the 750 °C (Fig. 8a) gasifier indicates four different carbon oxidation temperatures at 450 °C, 490 °C, 590 °C and 630 °C due to the presence of surface carbon to well-organized carbons such as iron carbide, filamentous carbon and/or carbon nanotubes.

The catalyst coming from the 800 °C (Fig. 8b) gasifier indicates only two main carbon oxidation temperatures at 585 °C and 630 °C.

By increasing the biomass gasification temperature, preferential formation of well-organized carbonaceous deposit is formed. No carbon oxidation peak is detected after 750 °C of the TPO measurements. Hence, under oxidative conditions of the combustor reactor (900 °C), the whole carbon deposited on the Fe/olivine catalyst surface is eliminated. Thus, explaining the catalyst stability.

4. Conclusion

The Fe/olivine catalyst efficiency was evaluated in biomass gasification in a dual fluidized bed for the production of a rich syngas and with low tar content. It has been found that Fe/olivine material has a double effect on tar destruction. On the one hand, it acts as a catalyst for tar and hydrocarbon reforming. On the other hand, it can act as an oxygen carrier that transfers oxygen from the combustor to the gasifier, and part of the oxygen is used to burn volatile compounds.

The characterization performed after the test indicates that the catalyst structure was maintained despite the large number of redox cycles (transition from an oxidizing zone to a reducing one). The carbon formed on the catalyst surface was low and easily oxidized in the combustion zone.

Therefore, an inexpensive and non-toxic Fe/olivine catalyst is a material suitable for use as a primary catalyst in a fluidized bed gasification of biomass and improves the commonly used olivine catalytic activity.

Acknowledgements

Authors would like to thank the European Commission for its financial support (EC Project UNIQUE N°211517-ENERGY FP7–2008/2011). http://www.uniqueproject.eu.

The Mössbauer study was supported by the Long-Term Research Plan of the Ministry of Education of the Czech Republic (MSM0021620857). Authors also express our gratitude to Daniel Schwartz for his help in the improvement of English of this paper.

References

[1] K. Maniatis, in: V. Bridgwater (Ed.), Progress in Biomass Gasification: An Overview, Blackwell Science, London, 2001, pp. 1–31.
[2] A. Gómez-Barea, B. Leckner, Progress in Energy and Combustion Science 36 (2010) 444–509.
[3] H. Hofbauer, H. Knoef, in: H.A.M. Knoef (Ed.), Handbook of Biomass Gasification, BTG Biomass Technology Group, Netherlands, 2005 (Chapter 6).
[4] T.A. Milne, R.J. Evans, N. Abatzoglou, Biomass gasifier "tars": their nature, formation, and conversion. National Renewable Energy Laboratory Report 1998, NREL/TP-570-23357.
[5] S. Anis, Z.A. Zainal, Renewable & Sustainable Energy Reviews 15 (2011) 2355–2377.
[6] H.A.M. Knoef, Handbook of Biomass Gasification, BTG Biomass Technology Group, Netherlands, 2005.
[7] M.M. Yung, K.A. Magrini-Bair, Y.O. Parent, D.L. Carpenter, C.J. Feik, K.R. Gaston, M.D. Pomeroy, S.D. Phillips, Catalysis Letters 134 (2010) 242–249.
[8] K.A. Magrini-Bair, S. Czernik, R. French, Y.O. Parent, E. Chornet, D.C. Dayton, C. Feik, R. Bain, Applied Catalysis A: General 318 (2007) 199–206.
[9] S. Rapagnà, N. Jand, A. Kiennemann, P.U. Foscolo, Biomass and Bioenergy 19 (2000) 187–197.
[10] D. Swierczynski, S. Libs, C. Courson, A. Kiennemann, Applied Catalysis B: Environmental 27 (2007) 211–222.
[11] C. Pfeifer, H. Hofbauer, R. Rauch, Industrial and Engineering Chemistry Research 43 (2004) 1634–1640.
[12] R. Rauch, C. Pfeifer, K. Bosch, H. Hofbauer, D. Swierczynski, C. Courson, A. Kiennemann, in: A.V. Bridgwater, D.G.B. Boocock (Eds.), Comparison of Different Olivines for Biomass Steam Gasification, CPL Press, UK, 2006, pp. 799–809.
[13] M. Virginie, C. Courson, D. Niznansky, N. Chaoui, A. Kiennemann, Applied Catalysis B: Environmental 101 (2010) 90–100.
[14] D. Swierczynski, C. Courson, L. Bedel, A. Kiennemann, S. Vilminot, Chemistry of Materials 18 (2006) 897–905.
[15] P. Simell, P. Ståhlberg, E. Kurkela, J. Albrecht, S. Deutsch, K. Sjöström, Biomass and Bioenergy 18 (2000) 19–38.
[16] D. Swierczynski, C. Courson, L. Bedel, A. Kiennemann, J. Guille, Chemistry of Materials 18/17 (2006) 4025–4032.

[17] L. Devi, M. Craje, P. Thune, K.J. Ptasinski, F.J.J.G. Janssen, Applied Catalysis A: General 294 (2005) 68–79.
[18] J.N. Kuhn, Z. Zhao, L.G. Felix, R.B. Slimane, C.W. Choi, U.S. Ozkan, Applied Catalysis B: Environmental 81 (2008) 14–26.
[19] R. Rauch, K. Bosch, H. Hofbauer, D. Swierczynski, C. Courson, A. Kiennemann, in: A.V. Bridgwater, D.G.B. Boocock (Eds.), Science in Thermal and Chemical Biomass Conversion, CPL Press, 2006, pp. 799–809.
[20] S. Rapagnà, M. Virginie, K. Gallucci, C. Courson, M. Di Marcello, A. Kiennemann, P.U. Foscolo, Catalysis Today 176 (2011) 163–168.
[21] C. Rodes, G.J. Hutchings, A.M. Ward, Catalysis Today 23 (1995) 43–58.
[22] K. Matsuoka, T. Shimbori, K. Kuramoto, H. Hatano, Y. Suzuki, Energy and Fuels 20 (2006) 2727–2731.
[23] J. Yu, F.J. Tian, L.J. McKenzie, C.Z. Li, Process Safety and Environment Protection 84 (2006) 125–139.
[24] A. Uddin, H. Tsuda, S. Wu, E. Sasaok, Fuel 87 (2008) 451–459.
[25] A. Orìo, J. Corella, I. Narvàez, Industrial and Engineering Chemistry Research 36 (1997) 3800–3808.
[26] T. Wang, J. Chang, P. Lv, Energy and Fuels 19 (2005) 22–27.
[27] S. Koppatz, T. Pröll, C. Pfeifer, H. Hoffbauer, Investigation of reforming activity and oxygen transfer of olivine in dual circulating fluidized bed system with regard to biomass gasification, in: Proceeding of Fluidization XIII Conference, Korea, 2010, p. 901.
[28] J. Adánez, A. Abad, F. García-Labiano, P. Gayán, L.F. de Diego, Progress in Energy and Combustion Science 38 (2012) 215–282.
[29] M. Virginie, C. Courson, A. Kiennemann, Comptes Rendus Chimie 13 (2010) 1319–1325.
[30] M. Virginie, «Élaboration et développement d'un catalyseur Fe/olivine pour le vaporeformage de molécules modèles de goudrons formés lors de la gazéification de la biomasse», Thesis, Strasbourg University, 2011.
[31] S.S. Tamhankar, K. Tsuchiya, J.B. Riggs, Applied Catalysis 16 (1985) 103–121.
[32] P.A. Simell, J.K. Leppälahti, J.B. Bredenberg, Fuel 71 (1992) 211–218.
[33] L. Di Felice, C. Courson, D. Niznansky, P.U. Foscolo, A. Kiennemann, Energy and Fuels 24 (2010) 4034–4045.
[34] T. Nordgreen, T. Liliedahl, K. Sjöström, Energy and Fuels 20 (2006) 890–895.
[35] K. Barcova, M. Mashlan, R. Zboril, P. Martinec, Journal of Radioanalytical and Nuclear Chemistry 255 (2003) 529–533.
[36] M. Morozov, C. Brinkmann, M. Grodzicki, W. Lottermoser, G. Tippelt, G. Amthauer, H. Kroll, Hyperfine Interactions 166 (2005) 573–578.
[37] E. Murad, J.H. Jonhson, in: G.J. Long (Ed.), Iron Oxides and Oxyhydroxides, Plenum, New York, 1987, pp. 507–582.
[38] H.H. Hamdeh, Z. Xia, R. Foehrweiser, B.J. McCormick, R.J. Willey, G. Busca, Journal of Applied Physics 76 (1994) 1135–1140.
[39] T. Fujii, M. Takano, R. Katano, Y. Isozumi, Y. Bando, Journal of Magnetism and Magnetic Materials 130 (1994) 267–274.
[40] F.J. Pérez-Alonso, M. Ojeda, T. Herranz, J.M. González-Carballo, J.L.G. Fierro, J.F. Bengoa, S.G. Marchetti, Open Magnetic Resonance Journal 1 (2008) 64–70.
[41] U. Nitzan, Journal of Geophysics Researches 79 (1974) 706–711.
[42] P.E. Champness, Mineralogical Magazine 37/291 (1970) 790–800.
[43] L. Di Felice, C. Courson, P.U. Foscolo, A. Kiennemann, International Journal of Hydrogen Energy 36 (2011) 5296–5310.
[44] K. Polychronopoulou, A. Bakandritsos, V. Tzitzios, J.L.G. Fierro, A.M. Efstathiou, Journal of Catalysis 241 (2006) 132–148.
[45] S. Fukase, T. Suzuka, Applied Catalysis A: General 100 (1993) 1–17.
[46] T. Nordgreen, K. Sjöström, T. Liliedahl, Fuel 85 (2006) 689–694.